



Numerical studies on dispersion of thermal waves



Min-Kai Zhang, Bing-Yang Cao*, Yin-Cheng Guo

Department of Engineering Mechanics, Tsinghua University, Beijing 100084, China

ARTICLE INFO

Article history:

Received 25 March 2013

Received in revised form 13 August 2013

Accepted 30 August 2013

Keywords:

Thermal wave

Dispersion

Cattaneo–Vernotte model

Dual-phase-lagging model

Thermomass model

ABSTRACT

Heat may transport as waves under ultrafast heat pulse conditions. In this paper, our numerical analyses considering typical thermal wave modes, i.e. Cattaneo–Vernotte (CV), dual-phase-lagging (DPL), and thermomass (TM), disclose that dispersion may occur during the heat propagation processes like water, sound, and light waves. The unified implicit finite difference method for the Fourier, CV, DPL, and TM models was adopted to analyze the heat propagation process in solids. The validity of this numerical method for the Fourier, CV, DPL and TM models was confirmed. The dispersion of thermal waves was observed in their propagation processes for the first time. As the thermal waves moving forward, many peaks appear in the rear of the thermal waves relative to the propagation direction. The underlying mechanism for the dispersion of the thermal waves is that they can travel faster in the points with higher temperature considering the temperature dependence of the relaxation time. For the CV-waves and DPL-waves, the origins of the dispersion are both due to the inertia term of heat flux to time ($\tau_q \frac{\partial q}{\partial t}$). For the TM-waves, the origins are due to the inertia term of heat flux to time, inertia term of temperature to time, and inertia term of heat flux to space in the TM model, and effects of the inertia term of temperature to space on the dispersion can be neglected, where the inertia term to space comes from the nonlocal effects. The dispersion of the TM-waves is mainly dominated by the inertia term of heat flux to time. In the TM model, the characteristic time τ_{TM} decreases with the increase of temperature, and therefore the dispersion will appear in the propagation process of the TM-wave. For actual materials, if considering that τ_q decreases with the temperature increasing, the dispersion of the CV-wave and DPL-wave will also appear under the appropriate amplitude of heat flux pulse, relaxation times τ_q and τ_r . The increase of the amplitude of heat flux pulse and the decrease of the initial temperature both can enhance the dispersion of the TM-wave. The increase of the amplitude of heat flux pulse and the relaxation time τ_q can both enhance the dispersion of the CV-wave and DPL-wave, while the increase of the relaxation time τ_r will weaken the dispersion of the DPL-wave.

© 2013 Elsevier Ltd. All rights reserved.

1. Introduction

As water, sound, and light waves of different wavelengths travel at different phase speeds, dispersion will occur in the wave propagation processes. For heat conduction in solids, it has been widely interpreted as diffusive, thermal wave [1–5] or ballistic phenomena [6–8]. Considering the thermal wave (second sound wave) in super fluid helium (He II) under strong heat flux perturbation, numerical results obtained by the Landau's two-fluid model indicated that the rear portion of a rectangular thermal wave expands gradually due to that wave travels faster in regions with higher temperature [9]. Therefore, when the heat propagation is in a wave mode, the dispersion may appear in the propagation process under appropriate initial-boundary conditions if the thermal waves propagate at different speeds. Understanding the dispersion of thermal waves may greatly benefit the ultrafast laser, high-frequency

circuit, ultralow temperature technologies and so on. However, reports on the thermal wave dispersion remain seldom thus far.

Typical heat conduction models which are most studied and applied include the Fourier model [10], Cattaneo–Vernotte (CV) model [11–13], dual-phase-lagging (DPL) model [2,14,15], and thermomass (TM) model [16–18] are shown in Eqs. (1)–(4), respectively,

$$\mathbf{q} = -k\nabla T, \quad (1)$$

$$\mathbf{q} + \tau_q \frac{\partial \mathbf{q}}{\partial t} = -k\nabla T, \quad (2)$$

$$\mathbf{q} + \tau_q \frac{\partial \mathbf{q}}{\partial t} = -k \left[\nabla T + \tau_r \frac{\partial (\nabla T)}{\partial t} \right], \quad (3)$$

$$\begin{aligned} \mathbf{q} + \tau_{TM} \frac{\partial \mathbf{q}}{\partial t} - \tau_{TM} \frac{\mathbf{q}}{T} \frac{\partial T}{\partial t} + \tau_{TM} \frac{\mathbf{q}}{\rho C_v T} \nabla \cdot \mathbf{q} - \tau_{TM} \frac{\mathbf{q}}{\rho C_v T} \cdot \frac{\mathbf{q}}{T} \nabla T \\ = -k\nabla T. \end{aligned} \quad (4)$$

* Corresponding author. Tel./fax: +86 10 6278 1610.

E-mail address: caoby@tsinghua.edu.cn (B.-Y. Cao).

Nomenclature

A	dimensionless amplitude of heat flux
C_v	specific heat, J/kg K
d	thickness, m
k	thermal conductivity, W/m K
q	heat flux, W/m ²
t	time, s
t_p	heat flux pulse duration, s
Δt	time step, s
T	temperature, K
T_0	initial temperature, K
V	thermal wave propagation speed, m/s
x	position, m
Δx	spatial step, m
Z	dimensionless relaxation time

Greek symbols

α	thermal diffusivity, $k/\rho \cdot C_v$, m ² /s
γ	Grüneisen constant
ρ	density, kg/m ³

τ	relaxation time, s
--------	--------------------

Superscript

*	dimensionless parameter
---	-------------------------

Subscripts

0	initial temperature
n	n -th step
p	heat flux pulse
q	heat flux
$q-t$	heat flux to time
$q-x$	heat flux to space
T	temperature
$T-t$	temperature to time
$T-x$	temperature to space
TM	thermomass
TMO	thermomass at initial temperature
v	volume

In Eqs. (1)–(4), q is the heat flux, T is the temperature, t is the time, and k is the thermal conductivity. Besides, in Eqs. (2) and (3), τ_q is the relaxation time of heat flux, which is defined as the ratio of the mean free path of phonons to their group speed and represents the time necessary for the initiation of the heat flux after a temperature gradient has been imposed. In Eq. (3), τ_T is the relaxation time of the temperature gradient (∇T) and represents the time necessary for the initiation of the temperature gradient established across the solid after the heat flux has been imposed. Both of the two relaxation times τ_q and τ_T are treated as intrinsic thermal or structural properties of the material. They are interpreted as being caused by the phonon collisions in a duration of the mean free time and the micro-structural interactions such as phonon-electron interaction or phonon scattering [19,20]. In Eq. (4), τ_{TM} is the lagging time for the thermal wave based on the thermomass theory, defined as $\alpha/(2\gamma C_v T)$, where α , i.e., $k/(\rho C_v)$, is the thermal diffusivity and γ is the Grüneisen constant. ρ and C_v are the mass density and heat capacity at constant volume of the solid, respectively. So, the initial lagging time $\tau_{TMO} = \alpha/(2\gamma C_v T_0)$ when $T = T_0$, where T_0 is the initial temperature. Except for the above heat conduction models, there are also many other models [21], especially when considering the nonlocal effects in a nonequilibrium steady state [22,23], such as the Guyer–Krumhansl model [24,25] and the nonlocal model proposed by Tzou and Guo [26].

The Fourier's law is valid for most engineering situations at the temporal and spatial macro scales although it assumes that thermal perturbation travels in solids at an unphysical infinite speed, which is in contradiction with the theory of relativity. But this diffusion model fails in situations such as the high-power under short durations like pulse-laser heating, micro-scale situations, cryogenic engineering and biological tissues due to its infinite heat propagation speed [27–31]. In the CV model, the introduction of τ_q leads to the finite CV-wave speed $\sqrt{\alpha/\tau_q}$ and this overcomes the limitation of the Fourier model. Therefore, the heat propagation process evolves from a diffusion to a wave phenomenon. The CV model can be reduced to the Fourier model when τ_q is negligible or when the time variation of heat flux is slow. But the CV model may give unphysical predictions such as negative temperature when two low-temperature cooling thermal waves meet [32,33]. Besides, the CV model assumes that an instantaneous heat flux within solids takes place right after the temperature gradient has been established across the solid, namely the temperature gradient is always the cause while the heat flux is

always the reason, which is actually untrue when considering the micro-structural interactions [34]. The DPL model considers both the inertia of the heat flux and the temperature gradient to time and can be reduced to the CV model when τ_T is negligible or when the time variation of temperature gradient is slow. For the case $\tau_q < \tau_T$, the temperature gradient established across the solid is a result of the heat flux, implying the heat flux is the cause and the temperature gradient is the result. But on the other hand, if $\tau_q > \tau_T$, the temperature gradient established at an earlier time, implying that the temperature gradient is the cause and the heat flux is the result. The DPL model includes four heat propagation modes: wave mode ($\tau_T = 0$), wavelike mode ($0 < \tau_T < \tau_q$), diffusion mode ($\tau_T = \tau_q$, since no lag phase exists between the heat flux and temperature gradient, which is the more general condition for reduction to the Fourier model in the absence of an initial variation of the temperature [16]), and over-diffusion mode ($\tau_T > \tau_q$) [35,36]. So, the propagation speed of the DPL-wave depends on both τ_q and τ_T [2], where the term “DPL-wave” only refers to the wavelike behavior of the DPL model. The TM model is based on the similarity between the phonon gas and the weighty, compressible fluid in consideration of that the heat conduction in dielectrics is seen as the motion of a “phonon gas”. By comparing Eqs. (2)–(4), it can be known that the TM model considers both the inertia of the heat flux and temperature to time and space while the CV model considers only the inertia of the heat flux to time and the DPL model considers the inertia of the heat flux and the temperature gradient to time, in which the inertia to space comes from the nonlocal effects. The propagation speed of the TM-wave is $q/(\rho C_v T) \pm \sqrt{\alpha/\tau_{TM}}$, i.e. $q/(\rho C_v T) \pm \sqrt{2\gamma C_v T}$, which is evidently a function of temperature within the solid.

According to the relationship between the relaxation time of heat flux and temperature for bulk silicon reported in Refs. [37,38], $1/\tau_q$ is proportional to cube of the temperature (i.e. $1/\tau_q \propto T^3$) while it is linear to temperature (i.e. $1/\tau_q \propto T$) when the temperature is higher than the Debye temperature. So, the CV-wave travels faster under higher temperature. This is also appropriate for the DPL model if assuming that the relaxation time of the temperature gradient τ_T keeps constant and does not change with temperature. For the TM-wave, considering the case $q/(\rho C_v T) \ll \sqrt{2\gamma C_v T}$, the propagation speed of the TM-wave is mainly dominated by $\sqrt{2\gamma C_v T}$, which indicates that the TM-wave

propagates faster when the temperature is higher. If the CV-wave, DPL-wave, and TM-wave propagate faster under higher temperature, the dispersion phenomena of these thermal waves may appear under the appropriate conditions in consideration of their similarities with water, sound, and light waves.

Extensive efforts have been devoted to analyze the propagation processes of thermal waves with analytical and numerical methods. For the analytical solutions, the most popular methods include the Laplace transform [26,39], Fourier series expansion [34,40,41], integral method [42,43] and Green's function [44,45]. Lam [34] carried out impressive work on the analytical methods and got the analytical solutions of the CV model, DPL model, and simplified TM model under time-varying and spatially-decaying laser incidences using the Fourier series expansion. But the analytical solutions in these works are only applicable to the specific formulations of initial-boundary conditions. Except the analytical methods, numerical methods can make good estimations on the propagation processes of thermal waves, especially when dealing with complex initial-boundary conditions. Torii and Yang [46] studied the overshooting phenomenon predicted by the CV model under the continuous-operated-laser and pulsating-laser heat sources with the MacCormack's predictor-corrector scheme and numerical results showed that the temperature overshooting phenomenon of the CV-wave depends on the frequency of the heat source. Xu et al. [47] also used numerical methods to study the mechanisms of the overshooting phenomenon predicted by the DPL model and pointed out that the thermal wave interference results in the overshooting phenomenon of temperature field and this phenomenon violates the second law of thermodynamics under the local equilibrium assumption. Ordonez-Miranda and Alvarado-Gil [48] used the numerical method to study the heat transport process governed by the CV model in a system formed by a finite layer in thermal contact with a semi-infinite layer under the Dirichlet and Neumann boundary conditions. Lam [49] used a concise finite difference algorithm based on the Godunov scheme to investigate the thermal propagation based on the CV model in solids due to surface laser pulsation and oscillation. Chou and Yang [50] used the space-time conversion element and solution element (CESE) method to study the propagation process of the DPL-waves through single-layer and multi-layer two-dimensional structures and found the wave, wavelike, diffusive and over-diffusive propagation mode within a single structure. Shen and Zhang [36] employed a purely numerical explicit total-variation-diminishing scheme to solve the DPL model under various initial-boundary conditions and the numerical solutions agreed well with the analytical solutions reported by Tzou [15]. Hu and Cao [32] adopted the explicit finite difference method to compared the thermal wave propagation processes predicted by the CV and TM models and found that the TM model can conquer the unphysical temperature under zero predicted by the CV model, which was later confirmed by Wang et al. [33].

In order to investigate the propagation processes of thermal waves predicted by the CV, DPL, and TM models, the present work employed an implicit finite difference method to solve the three heat conduction models, as well as the Fourier model, under a cosine heat flux pulse boundary condition. The dispersion of thermal waves in the propagation process was observed for the first time. The mechanisms and features of this phenomenon were studied. Effects of the amplitude of the heat flux pulse and initial temperature within solids on the dispersion of TM-waves were analyzed. Considering the relaxation times of heat flux τ_q in CV and DPL models decrease with the temperature increasing, the dispersion phenomena of the CV-waves and DPL-waves were also found. Effects of the amplitude of heat flux pulse and the relaxation time of heat flux τ_q and τ_T on the dispersion of CV-waves and DPL-waves were also studied in this work.

2. Numerical method

Considering a one-dimensional heat conduction problem such as the heat conduction in a thin film, the film was assumed finite in the x -direction while infinite in the y - and z -directions. A unified dimensionless method for the Fourier model, CV model, DPL model, and TM model was adopted. The dimensionless position x^* , time t^* , temperature T^* , heat flux q^* , and characteristic times Z_q , Z_T , Z_{TMO} are, respectively, defined as:

$$\begin{aligned} x^* &= x/d, \quad t^* = t/(d^2/\alpha), \quad T^* = T/T_0, \quad q^* = q/(kT_0/d), \\ Z_q &= \tau_q/(d^2/\alpha), \quad Z_T = \tau_T/(d^2/\alpha), \quad Z_{TMO} = \tau_{TMO}/(d^2/\alpha), \end{aligned} \quad (5)$$

where d is the thickness of the thin film. Z_q and Z_T are the dimensionless relaxation time of the heat flux and temperature gradient, respectively. Z_{TMO} is the dimensionless characteristic time in the TM model at the initial temperature T_0 .

The corresponding dimensionless expressions of the Fourier model Eq. (1), CV model Eq. (2), DPL model Eq. (3), and TM model Eq. (4) are, respectively, as follows

$$q^* + \frac{\partial T^*}{\partial x^*} = 0, \quad (6)$$

$$q^* + Z_q \frac{\partial q^*}{\partial t^*} + \frac{\partial T^*}{\partial x^*} = 0, \quad (7)$$

$$q^* + Z_q \frac{\partial q^*}{\partial t^*} + \frac{\partial T^*}{\partial x^*} + Z_T \frac{\partial^2 T^*}{\partial t^* \partial x^*} = 0, \quad (8)$$

$$q^* + \frac{Z_{TMO}}{T^*} \frac{\partial q^*}{\partial t^*} - \frac{Z_{TMO}}{T^*} \frac{q^*}{T^*} \frac{\partial T^*}{\partial t^*} + \frac{Z_{TMO}}{T^*} \frac{q^*}{T^*} \frac{\partial q^*}{\partial x^*} - \frac{Z_{TMO}}{T^*} \frac{q^*}{T^*} \frac{q^*}{T^*} \frac{\partial T^*}{\partial x^*} + \frac{\partial T^*}{\partial x^*} = 0. \quad (9)$$

To get the temperature distribution in the thin film under a heat flux pulse boundary, the energy conservation equation is also needed. Using the unified dimensionless units defined in Eq. (5), the dimensionless energy conservation equation with constant thermal properties and no heat sources is as follows

$$\frac{\partial T^*}{\partial t^*} + \frac{\partial q^*}{\partial x^*} = 0. \quad (10)$$

The implicit finite difference method was adopted to calculate the dimensionless temperature distributions at different instants of time. The spatial domain used the central difference while the time domain used the backward difference. Besides, considering the hyperbolic characteristic of the DPL and TM models, the mixed derivative term $Z_T \frac{\partial^2 T^*}{\partial t^* \partial x^*}$ in Eq. (8) and the inertia term of the heat flux to space $\frac{Z_{TMO}}{T^*} \frac{q^*}{T^*} \frac{\partial q^*}{\partial x^*}$ in Eq. (9) adopted the upwind scheme. The iteration process for the temperature reaches closure when the error criterion satisfies $|T_{n+1}^* - T_n^*| \leq 10^{-6}$.

3. Validation of the numerical method

Before presenting the dimensionless temperature distributions predicted by the Fourier, CV, DPL and TM models, we need to test the validity of the implicit finite difference method defined above in solving these heat conduction models. The implicit finite difference method for the Fourier model was also introduced and applied in Ref. [51] and its validity can be guaranteed by $\Delta t^*/\Delta x^{*2} \leq 0.5$, where Δt^* and Δx^* are the dimensionless time and spatial step in the numerical calculation, respectively. So, this numerical method can be regarded as valid for the Fourier model under the appropriate dimensionless time and spatial step.

One-dimensional heat conduction problem was considered to test the validity of this implicit finite difference method. When

testing the validity of this numerical method for the CV model and TM model, the same initial-boundary conditions as reported by Hu and Cao [32] were adopted, as defined in Eqs. (11)–(13):

$$T^* = 1 \text{ and } q^* = 0 \text{ at } t^* = 0, \quad (11)$$

$$T^* = 0.5 \text{ at } x^* = 0, t^* > 0, \quad (12)$$

$$T^* = 0.5 \text{ at } x^* = 1, t^* > 0. \quad (13)$$

But when testing the validity of this numerical method for the DPL model, the same initial-boundary conditions as reported by Shen and Zhang [36] were adopted, as defined in Eqs. (14)–(16):

$$T^* = 1 \text{ and } q^* = 0 \text{ at } t^* = 0, \quad (14)$$

$$q^* = 2 \text{ at } x^* = 0, t^* < 0.05 \text{ and } q^* = 0 \text{ at } x^* = 0, t^* \geq 0.05, \quad (15)$$

$$q^* = 0 \text{ at } x^* = 1, t^* > 0. \quad (16)$$

Besides, according to Ref. [32], Z_q in the CV model and Z_{TM0} in the TM model were both set 1.0. Also according to Ref. [36], Z_q and Z_T in the DPL model were set as 1.0 and 0.002, respectively.

Comparisons between the spatial dimensionless temperature distributions at $t^* = 0.4$ and $t^* = 1.2$ predicted by the CV model and TM model using the present numerical method and the numerical solution reported by Hu and Cao [32] are shown in Figs. 1 and 2, respectively. Meanwhile, comparison between the spatial dimensionless temperature distributions at $t^* = 0.4$ and $t^* = 1.4$ predicted by the DPL model using the present numerical method and the numerical solution reported by Shen and Zhang [36] is shown in Fig. 3. From Figs. 1–3, it can be seen that the present numerical solutions are in good agreement with the numerical solution reported by Hu and Cao [32] and Shen and Zhang [36]. The small discord is due to the numerical oscillation in the vicinity of sharp temperature gradient or discontinuities [52], which is also reported in Refs. [32,46]. From the comparisons above-mentioned, we can conclude that this implicit finite difference method is valid in solving the Fourier model, CV model, DPL model, and TM model. So, this implicit finite difference method can be used to study the dispersion of thermal waves. Besides, it is fairly obvious that the heat flux pulse boundary condition is more effective than the constant temperature boundary condition when studying how the thermal waves propagate in solids and this is especially important when analyzing the changing processes of the amplitudes and speeds of thermal waves quantitatively.

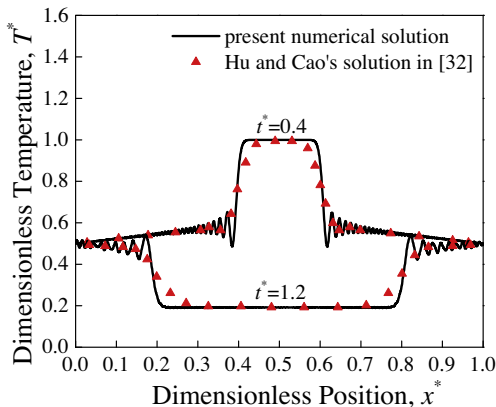


Fig. 1. Comparison between the spatial dimensionless temperature distributions at $t^* = 0.4$ and $t^* = 1.2$ predicted by the CV model using the present numerical method and the numerical solution reported by Hu and Cao [32].

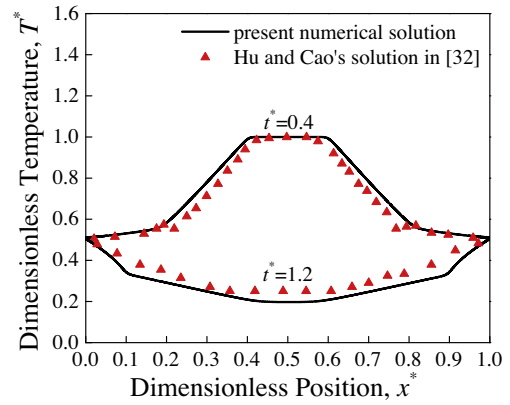


Fig. 2. Comparison between the spatial dimensionless temperature distributions at $t^* = 0.4$ and $t^* = 1.2$ predicted by the TM model using the present numerical method and the numerical solution reported by Hu and Cao [32].

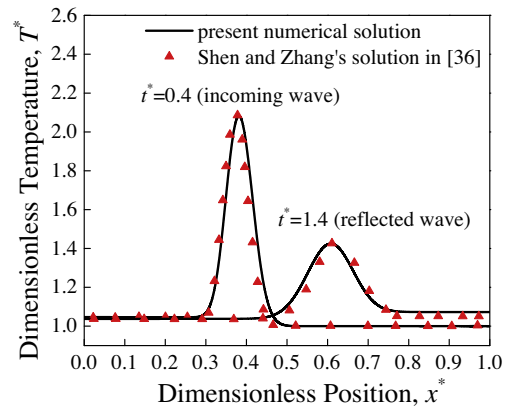


Fig. 3. Comparison between the spatial dimensionless temperature distributions at $t^* = 0.4$ and $t^* = 1.4$ predicted by the DPL model using the present numerical method and the numerical solution reported by Shen and Zhang [36].

4. Physical model

Considering a one-dimensional thin film as shown in Fig. 4, the thin film is finite in the x -direction while infinite in the y - and z -directions. The initial-boundary conditions are given as follows

$$T^* = 1 \text{ and } q^* = 0 \text{ at } t^* = 0, \quad (17)$$

$$q^* = A[1 - \cos(2\pi t^*/t_p^*)] \text{ at } x^* = 0, t^* < t_p^* \text{ and } q^* = 0 \text{ at } x^* = 0, t^* \geq t_p^*, \quad (18)$$

$$q^* = 0 \text{ at } x^* = 1, t^* > 0. \quad (19)$$

where A and t_p^* are the dimensionless amplitude and duration of the cosine heat flux pulse, respectively, which were also determined using the unified dimensionless method defined in Eq. (5). So, the heat flux pulse can be changed according to the actual research topic by adjusting the dimensionless amplitude A and pulse duration t_p^* . For an example, we can enhance the thermal perturbation by increasing the dimensionless amplitude A of the cosine heat flux pulse.

Before presenting the numerical solutions, a unified base condition for these heat conduction models needs to be introduced first. For the cosine heat pulse, the dimensionless amplitude A and pulse duration t_p^* were both set as 0.1 except for particular instructions. The thickness, initial temperature and relevant thermal properties

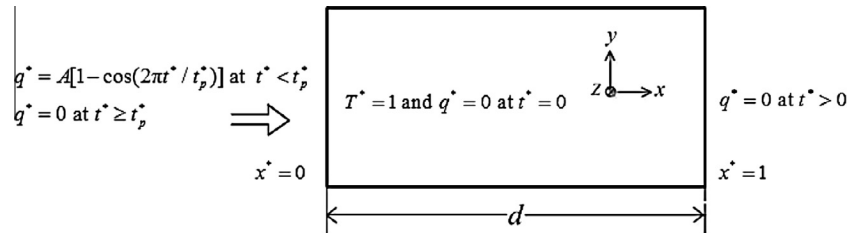


Fig. 4. Schematic diagram for a one-dimensional heat conduction problem under a cosine heat flux pulse boundary condition.

of the thin film also need to be defined. The thickness d of the thin film was set as 1.0. The initial temperature T_0 of the thin film was set as 1.0. The thermal conductivity k , mass density ρ , heat capacity C_v at constant volume, Grüneisen constant γ were also all set as 1.0, respectively. So, the characteristic time τ_{TM0} in the TM model was 0.5 at the initial temperature T_0 . The relaxation time of heat flux τ_q was set as 1.0, which was assumed same in the CV model and DPL model. In order to study the propagation process of the DPL-wave, the relaxation time of temperature gradient τ_T in the DPL model needed to be smaller than τ_q , and was set as 0.01. The length and thermal properties mentioned above were all assumed constant in the heat propagation process except for particular instructions. Therefore, the dimensionless characteristic times Z_q, Z_T, Z_{TM0} in the CV model, DPL model and TM model are 1.0, 1.0, and 0.5, respectively.

5. Results and discussion

5.1. Comparison of the dimensionless temperature distributions predicted by the Fourier, CV, DPL and TM models

Under the base conditions defined in Section 4 and the initial-boundary conditions defined in Eqs. (17)–(19), the spatial dimensionless temperature distributions at different instants of time predicted by the Fourier model, CV model, DPL model, and TM model are shown in Fig. 5(a)–(d), respectively. From Fig. 5, it can be seen that the heat propagation process predicted by the Fourier model behaves in a diffusive mode while the heat propagation processes predicted by the other three models behave in a wave mode. For the heat conduction models other than the Fourier model, such as the CV model, DPL model, and TM model, the temperature of some inner regions in the solid may exceed the temperature at the boundary and this is called an overshooting phenomenon, which was also reported by Xu et al. [47]. The overshooting phenomenon violates the second law of thermodynamics under the local equilibrium assumption [27,47], which means that the local equilibrium assumption is not applicable for the CV DPL and TM models. Under this condition, the energy might even transfer in the direction of increasing temperature [36]. It is worthwhile to mention that the overshooting phenomenon has been explained successfully by the extended irreversible thermodynamics (EIT) theory [27,30]. This nonlocal behavior in thermal lagging of the TM model explains the temperature of some inner regions in the film at $t^* = 0.7$ exceeds that at earlier time due to the heating by other inner regions, as shown in Fig. 5(d).

Comparing to the CV model, the introduction of the relaxation time of temperature gradient τ_T in the DPL model enhances the heat diffusion of the DPL-wave. So, at the same instants of time, the peak temperatures of the DPL-waves are lower than those of the CV-waves and the DPL-waves are also less sharp than the CV-waves, as shown in Fig. 5(b) and (c). At the beginning time $t^* = 0.1$, the peak temperature of the TM-wave is also lower than that of the CV-wave and the TM-wave is also less sharp than the CV-wave. This is because the characteristic time τ_{TM} in the TM

model is smaller than the relaxation time of heat flux τ_q in the CV model and thus making the heat diffusion stronger in the TM-wave, which gives rise to the lower peak temperatures of the TM-waves.

In Fig. 5(a), as the heat propagation speed in the Fourier model is infinite, the dimensionless temperature within the thin film decreases to 1.01 rapidly. In Fig. 5(b), the amplitude of the dimensionless temperature predicted by the CV model decreases gradually along with the CV-wave propagating due to the heat diffusion. Because of the relaxation time τ_T , the heat diffusion in the DPL model is stronger than that in the CV model, and hence the propagation speed of the DPL-wave is faster than the CV-wave and the decay of the DPL-wave is more significant than that of the CV-wave. As the characteristic time τ_{TM} in the TM model is smaller than the relaxation time τ_q in the CV and DPL models, the propagation speed of the TM-wave is faster than those of the CV-wave and DPL-wave.

From Fig. 5(d), it can be seen that there is only one peak at the beginning of the TM-wave, but two peaks appear for the TM-wave at $t^* = 0.3$ and three peaks appears at $t^* = 0.5$. For the current conditions, this phenomenon does not appear in the CV-wave and DPL wave, but occurs in the TM-wave. The reason for this is that under the unified base conditions and dimensionless method, $q/(\rho C_v T)$ is at least an order of magnitude lower than $\sqrt{2\gamma C_v T}$, and hence the propagation speed of the TM-wave is mainly dominated by $\sqrt{2\gamma C_v T}$, which means the TM-wave travels faster in the points with higher temperature since the thermal properties remain constant. With the time going on, the TM-waves of different propagation speeds begin to disperse gradually. However, the propagation speeds of the CV-wave and DPL-wave both remain unchanged since the relaxation times τ_q and τ_T keep constant. As the dispersion is similar to the dispersion of water, sound, and light waves, we call this as the dispersion of thermal waves. Besides, as the propagation speed of the TM-wave is faster in the points with higher temperature while slower in the point with lower temperature, new peaks only appear in the rear of the TM-waves relative to the propagation direction.

5.2. Origin of the dispersion of TM-waves

The dispersion is due to the higher propagation speed of the TM-wave in the points with higher temperature. Comparing to the CV and DPL models, the inertia term of heat flux to time $\tau_{TM} \frac{\partial q}{\partial t}$, inertia term of temperature to time $\tau_{TM} \frac{q}{T} \frac{\partial T}{\partial t}$, inertia term of heat flux to space $\tau_{TM} \frac{q}{\rho C_v T} \nabla \cdot q$ and inertia term of temperature to space $\tau_{TM} \frac{q}{\rho C_v T} \cdot \frac{q}{T} \nabla T$ in the TM model are all possible origins for the dispersion, where the inertia term to space comes from the nonlocal effects. To analyze the effects of these inertia terms on the dispersion of the TM-waves, according to the CV model as shown in Eq. (2), the TM model in Eq. (4) can be correspondingly modified into Eqs. (20)–(23):

$$\mathbf{q} + \tau_{TM} \frac{\partial \mathbf{q}}{\partial t} = -k \nabla T, \quad (20)$$

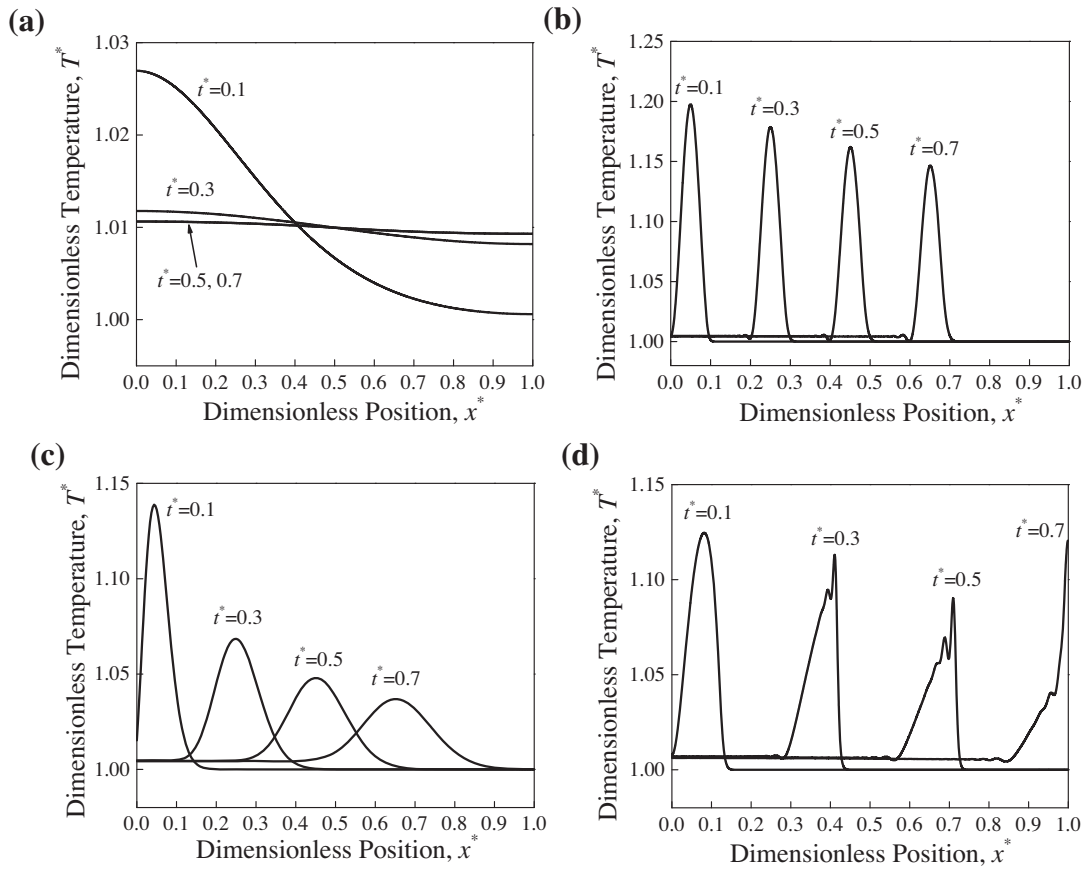


Fig. 5. The spatial dimensionless temperature distributions at different instants of time predicted by the (a) Fourier model, (b) CV model, (c) DPL model, and (d) TM model.

$$\mathbf{q} + \tau_{TM0} \frac{\partial \mathbf{q}}{\partial t} - \tau_{TM} \frac{\mathbf{q}}{T} \frac{\partial T}{\partial t} = -k \nabla T, \quad (21)$$

$$\mathbf{q} + \tau_{TM0} \frac{\partial \mathbf{q}}{\partial t} + \tau_{TM} \frac{\mathbf{q}}{\rho C_v T} \nabla \cdot \mathbf{q} = -k \nabla T, \quad (22)$$

$$\mathbf{q} + \tau_{TM0} \frac{\partial \mathbf{q}}{\partial t} - \tau_{TM} \frac{\mathbf{q}}{\rho C_v T} \nabla T = -k \nabla T. \quad (23)$$

For Eq. (20), we can study effects of the inertia term of heat flux to time on the dispersion of the TM-wave, as shown in Fig. 6(a). This inertia term is different from that of the CV model because the characteristic time τ_{TM} , i.e. $\alpha/(2\gamma C_v T)$, in Eq. (20) decreases with the temperature T increasing while τ_q in Eq. (2) stays unchanged in the propagation process of the CV-wave, and thus leading to faster thermal wave speed under higher temperature in Eq. (20). For Eqs. (21)–(23), we can study effects of the inertia term of temperature to time, inertia term of heat flux to space, inertia term of temperature to space, respectively. The propagation processes of thermal waves predicted by Eqs. (21)–(23) are shown in Fig. 6(b)–(d). It should be mentioned that in Eqs. (21)–(23), in order to avoid the interference of the inertia term of heat flux to time, τ_{TM} is compulsorily replaced by τ_{TM0} since the temperature T in the main region of the film is near the initial temperature T_0 . Besides, it is worthwhile to mention that according to the energy conservation equation $\rho C_v \frac{\partial T}{\partial t} + \nabla \cdot \mathbf{q} = 0$ with constant thermal properties and no heat sources, Eq. (21) can be transformed into Eq. (22) by replacing $\frac{\partial T}{\partial t}$ by $-\frac{\nabla \cdot \mathbf{q}}{\rho C_v}$, and therefore effects of the inertia term of temperature to time and effects of the inertia term of heat flux to space on the dispersion are same, as shown in Fig. 6(b) and (c).

According to Refs. [16,26], the thermal wave propagation speeds in Eqs. (20)–(23) are, respectively, as follows

$$V_{q-t} = \sqrt{2\gamma C_v T}, \quad (24)$$

$$V_{T-t} = \sqrt{2\gamma C_v T_0 + \left(\frac{q}{2\rho C_v T}\right)^2} + \frac{q}{2\rho C_v T} \quad (25)$$

$$V_{q-x} = \sqrt{2\gamma C_v T_0 + \left(\frac{q}{2\rho C_v T}\right)^2} + \frac{q}{2\rho C_v T} \quad (26)$$

$$V_{T-x} = \sqrt{2\gamma C_v T_0} \quad (27)$$

From Eq. (24), it can be seen that the wave propagation speed V_{q-t} is larger in the points with higher temperature. So, the dispersion appears in the wave propagation process when only considering the effects of heat flux to time, as shown in Fig. 6(a). In the thermal wave propagation process, the heat flux wave is in accord with the temperature wave [36], namely the heat flux is stronger in the points with higher temperature. But for the current conditions, the increase of temperature is less significant than that of heat flux, and therefore the wave propagation speeds V_{T-t} as shown in Eq. (25) and V_{q-x} as shown in Eq. (26) are mainly dominated by the heat flux and they are both faster in the points with higher temperature. Besides, from V_{q-x} defined in Eq. (26), we can know that the introduction of the nonlocal behavior leads to higher propagation speed than the CV-wave, which is also reported by Tzou [54]. In Ref. [54], Tzou not only considered the first-order nonlocal effect which was included in the TM model, but also considered the second-order nonlocal effect which was not included in the TM model. If

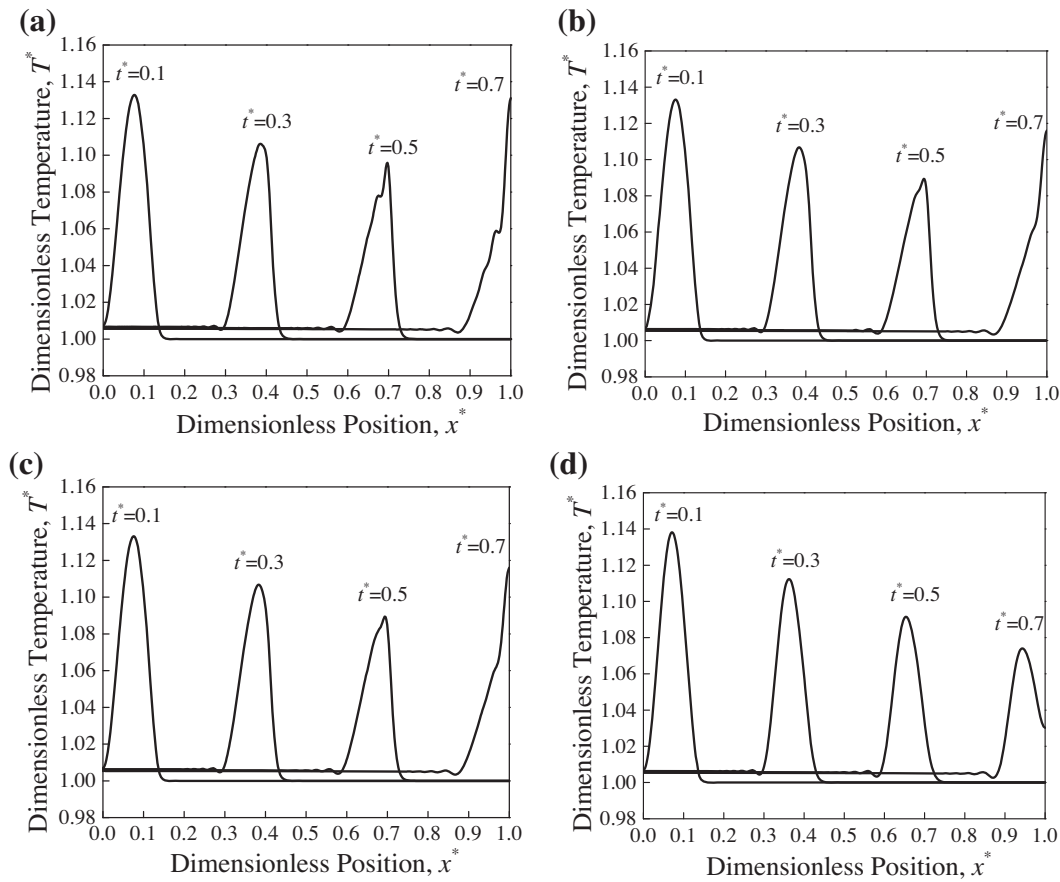


Fig. 6. Effects of (a) the inertia term of heat flux to time, (b) the inertia term of temperature to time, (c) the inertia term of heat flux to space, and (d) the inertia term of temperature to space in the TM model on the dispersion of TM-waves, where the inertia term to space comes from the nonlocal effects.

considering the second-order effects, it can effectively destroys the sharp wave front of the nonlocal waves, resulting in continuous distributions of temperature, like diffusion.

As defined in Section 4, the thermal conductivity k , mass density ρ , heat capacity C_v at constant volume, Grüneisen constant γ and initial temperature T_0 were all set as 1.0 in this paper. So, combining the unified dimensionless units defined in Eq. (5) and the situation that the dimensionless heat flux is at least one order of magnitude lower than the dimensionless temperature in this paper, we can know that the change of V_{T-t} and V_{q-x} with heat flux is less significant than that of V_{q-t} with temperature. As a whole, the dispersion phenomena when analyzing the effects of the inertia term of temperature to time and the effects of the inertia term of heat flux to space are both less significant than that when analyzing only the effects of the inertia term of heat flux to time, which can be seen by comparing with the thermal waves in Fig. 6(a)–(c). The thermal wave propagation speed V_{T-x} in Eq. (27) is constant and smaller than other three wave speeds V_{q-t} , V_{T-t} , V_{q-x} , as shown in Eqs. (24)–(26). So, the dispersion does not occur in the wave propagation process when only considering the effects of the inertia term of temperature to space and the thermal wave in Fig. 6(d) travels more slowly than the other three thermal waves in Fig. 6(a)–(c). Since the unmodified TM model includes effects of the four inertia terms analyzed above, the dispersion predicted by the unmodified TM model is more significant than those when only analyzing the effects of only one of the inertia terms, which can be seen by comparing with the thermal waves in Figs. 5d and 6(a)–(c).

In a summary, the underlying mechanism for the dispersion of the TM-waves is that they can travel faster in the points with

higher temperature considering the temperature dependence of the relaxation time. The origins of this phenomenon are due to the inertia term of heat flux to time, inertia term of temperature to time and inertia term of heat flux to space in the TM model. Effects of the inertia term of temperature to space on the dispersion can be neglected. The dispersion of the TM-waves is mainly dominated by the inertia term of heat flux to time. Besides, according to the energy conservation, it can be inferred that the deeper reason for the appearance of the temperature peaks is that the energy is transported into the corresponding region. Meanwhile, the appearance of the temperature troughs is due to the energy transported out. Therefore, the temperature peaks and troughs are similar to the focusing and defocusing of heat pluses along nonequilibrium nanowires reported by Jou and Sellitto [53].

5.3. Effects of the amplitude of heat flux pulse and initial temperature on the dispersion of TM-waves

Fig. 7 shows the effects of the amplitude of the heat flux pulse and initial temperature on the dispersion of the TM-waves. As shown in Fig. 7(a), the peak temperatures of TM-waves increase significantly with increasing the amplitude of heat flux pulse and meanwhile the dispersion of the TM-waves is more obvious under higher amplitude of heat flux pulse since the difference of TM-wave propagation speeds under stronger heat flux perturbation is more significant. The propagation speed of the TM-wave is larger when $A = 0.12$ than that when $A = 0.03$ since the temperature difference in the thin film is higher under higher amplitude of heat flux pulse. When the dimensionless amplitude A is 0.03, the

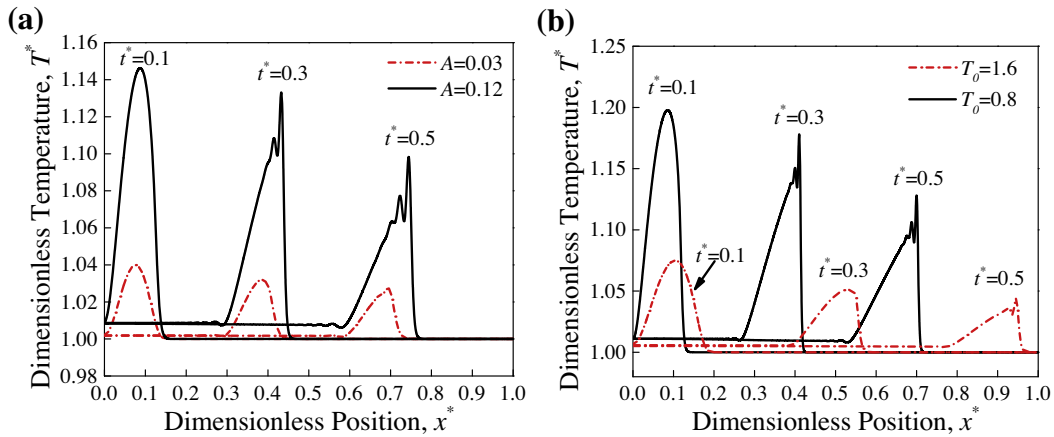


Fig. 7. Effects of (a) the amplitude of heat flux pulse and (b) the initial temperature of the thin film on the dispersion of TM-waves.

dispersion almost does not appear in the range of computing time. As shown in Fig. 7(b), the TM-waves travel faster under higher initial temperature, but the dispersion is very weak and only appears at $t^* = 0.5$ when $T_0 = 1.6$. This is because when $T_0 = 1.6$, the global temperature within the film is higher and therefore the characteristic time τ_{TM} in the TM model is smaller, which leads to stronger heat diffusion. As the heat diffusion is stronger when $T_0 = 1.6$, the peak temperatures are lower than those when $T_0 = 0.8$. So, when the initial temperature is sufficiently high, the thermal waves will not be detected, which is in accord with the experimental results that the thermal wave phenomena were mainly observed in the cryogenic environment [2,9]. But if the relaxation times τ_q and τ_T in the CV model and DPL model are both assumed constant and does not change with temperature, the effects of the initial temperature on the thermal waves will only exist in the TM model because the relaxation time τ_{TM} , as well as the propagation speed of the TM-wave, greatly depends on the temperature. As shown in Fig. 7(a) and (b), as the TM-waves move forward, they all become unsymmetrical gradually with the wave front leaning to the heat propagation direction, which was also reported by Guo and Hou [16].

5.4. Dispersion phenomena of CV-waves and DPL-waves

In the CV and DPL models, the relaxation time of heat flux τ_q is the ratio of the mean free path of phonons to the group speed. τ_q was assumed constant in most previous work [32–34,36,47,48] although it is actually affected by the temperature in actual materials. According to the relationship between the relaxation time of heat flux and temperature for bulk silicon reported in Refs. [37,38], $1/\tau_q$ is proportional to cube of the temperature (i.e. $1/\tau_q \propto T^3$) while the dependence is linear to temperature (i.e. $1/\tau_q \propto T$) when the temperature is higher than the Debye temperature. Here, we take $Z_q = 0.3/T^*$ and $Z_q = 0.3/T^{*3}$ for example to investigate whether the dispersion will appear in the propagation processes of the CV-wave and DPL-wave. The dimensionless relaxation time of temperature gradient Z_T in the DPL model is set as 10^{-5} , which stayed unchanged in the propagation process of the DPL-wave. Besides, the dimensionless amplitude of heat flux pulse A was set as 0.1, same with the base conditions.

The spatial dimensionless temperature distributions at different instants of time predicted by the CV and DPL models under the conditions $Z_q = 0.3/T^*$ and $Z_q = 0.3/T^{*3}$ are shown in Fig. 8. Since $(0.3/T^*) > (0.3/T^{*3})$, the peak temperatures of the CV-waves and DPL-waves are higher when $Z_q = 0.3/T^*$ at $t^* = 0.1$. But at $t^* = 0.3$ and $t^* = 0.5$, it does not hold because some inner regions can obtain

energy from other regions where the temperature is lower, which is also caused by the nonlocal behavior in thermal lagging. For the current conditions, the dispersion appears in the CV-waves and DPL-waves when $Z_q = 0.3/T^{*3}$, but does not appear when $Z_q = 0.3/T^*$ in the range of computing time. This is because effects of the temperature on the relaxation time τ_q are more significant when $Z_q = 0.3/T^{*3}$ than that when $Z_q = 0.3/T^*$, and thus leading to the differences of thermal wave propagation speeds are more significant when $Z_q = 0.3/T^{*3}$. According to the effects of the amplitude of heat flux pulse and initial temperature on the dispersion in Section 4.3, for $Z_q = 0.3/T^*$, the increase of amplitude of heat flux or the relaxation time τ_q itself may lead to the appearance of dispersion in the range of computing time and this will be presented in the following sections. So, for the CV-waves and DPL-waves, the origins of the dispersion are both the inertia term of heat flux to time ($\tau_q \frac{\partial q}{\partial t}$). Besides, under the conditions $Z_q = 0.3/T^*$ and $Z_q = 0.3/T^{*3}$, as the CV-waves and DPL-waves move forward, they all become unsymmetrical gradually with the wave fronts leaning to the heat propagation direction. This trend is same with the TM-waves since the CV-waves and DPL-waves both travel faster under higher temperature when considering that the relaxation time of heat flux τ_q decreases with temperature.

5.5. Effects of the amplitude of heat flux pulse on the dispersion of CV-waves and DPL-waves

Fig. 9 shows the effects of the amplitude of heat flux pulse on the dispersion of the CV-waves and DPL-waves under the conditions $Z_q = 0.3/T^*$ and $Z_T = 10^{-5}$. With the dimensionless amplitude of heat flux pulse A increasing, the peak temperatures of the CV-waves and DPL-waves both increase significantly. When $A = 0.2$, the dispersion of the CV-waves and DPL-waves appear at $t^* = 0.5$. But for the current conditions, the dispersion does not appear when $A = 0.1$. This trend is same with the dispersion of the TM-waves. Therefore, under the condition $Z_q = 0.3/T^*$, in the range of computing time, the dispersion can also appear in the propagation process of CV-waves and DPL-waves if the heat flux pulse perturbation is sufficiently strong. Besides, it can be seen that at $t^* = 0.5$, the dispersion of the CV-waves is more obvious than that of the DPL-waves because the relaxation time of temperature gradient τ_T in the DPL model enhances the heat diffusion of the DPL-waves.

5.6. Effects of τ_q and τ_T on the dispersion of CV-waves and DPL-waves

Fig. 10 shows the effects of the relaxation time of heat flux τ_q on the dispersion of the CV-waves and DPL-waves under the

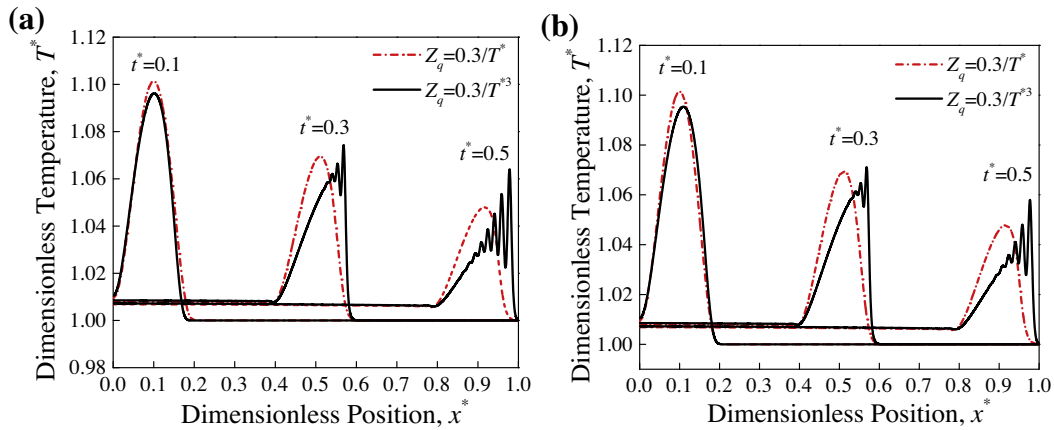


Fig. 8. The spatial dimensionless temperature distributions at different instants of time predicted by the (a) CV model and (b) DPL model under the conditions $Z_q = 0.3/T^*$ and $Z_q = 0.3/T^{*3}$, where $Z_T = 10^{-5}$ in the DPL model.

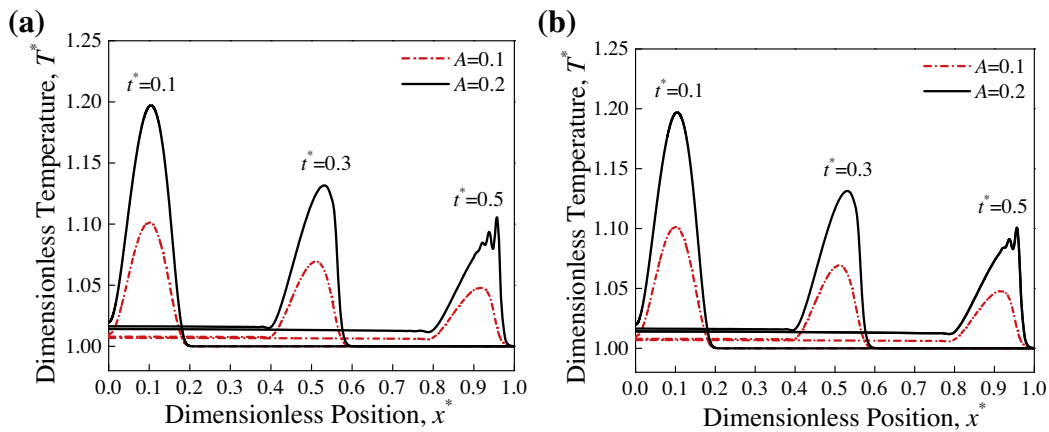


Fig. 9. Effects of the amplitude of heat flux pulse on the dispersion of (a) CV-waves and (b) DPL-waves under the condition $Z_q = 0.3/T^*$ and $Z_T = 10^{-5}$.

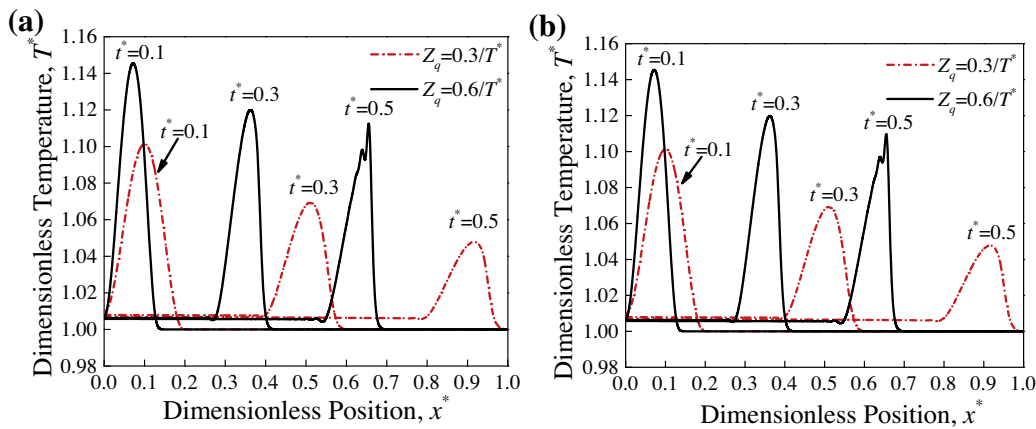


Fig. 10. Effects of the relaxation time of heat flux τ_q on the dispersion of (a) CV-waves and (b) DPL-waves under the conditions $Z_q = 0.3/T^*$ and $Z_q = 0.6/T^*$, where $Z_T = 10^{-5}$ in the DPL model.

conditions $Z_q = 0.3/T^*$ and $Z_q = 0.6/T^*$, where $Z_T = 10^{-5}$ in the DPL model. The dimensionless amplitude of heat flux pulse A was set as 0.1. The heat diffusion in the CV and DPL models when $Z_q = 0.6/T^*$ is both weaker than that when $Z_q = 0.3/T^*$, and thus giving rise to faster propagation speeds, higher peak temperatures of the thermal waves, more sharp thermal waves and more obvious dispersion when $Z_q = 0.6/T^*$. For the current conditions, when

$Z_q = 0.3/T^*$, the dispersion of the CV-waves and DPL-waves does not occur in the range of computing time and this phenomenon can occur when using larger amplitude of heat flux pulse or relaxation time τ_q . This trend is also same with the dispersion of the TM-waves because when the dispersion of the TM-waves is also weaker under higher initial temperature due to the smaller characteristic time τ_{TM} in the TM model under higher temperature.

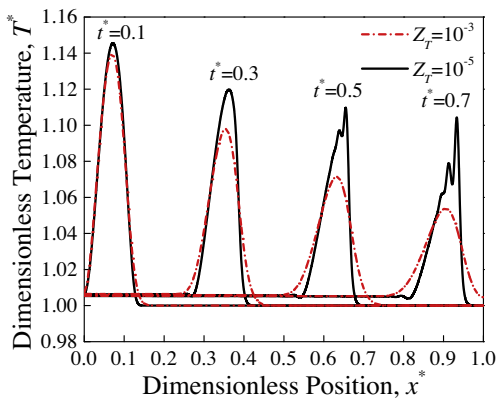


Fig. 11. Effects of the relaxation time of the temperature gradient τ_T on the dispersion of the DPL-waves under the conditions $Z_T = 10^{-3}$ and $Z_T = 10^{-5}$, where $Z_q = 0.6/T^*$ in the DPL model.

Fig. 11 shows the effects of the relaxation time of the temperature gradient τ^T on the dispersion of the DPL-waves under the conditions $Z_T = 10^{-3}$ and $Z_T = 10^{-5}$, where $Z_q = 0.6/T^*$ in the DPL model. The dimensionless amplitude of heat flux pulse A was set as 0.1. The increase of the relaxation time τ_T leads to stronger heat diffusion, and thus leading to faster propagation speed, lower peak temperatures of the DPL-waves and less sharp DPL-waves. When $Z_T = 10^{-3}$, the dispersion of the DPL-waves does not occur in the range of computing time. Therefore, the dispersion of the DPL-waves can be dominated by the amplitude of heat flux pulse, the relaxation time of heat flux τ_q and the relaxation time of the temperature gradient τ_T . The increase of the amplitude of heat flux pulse and the relaxation time τ_q can both enhance the dispersion. But, on the contrary, the increase of the relaxation time τ_T will weaken the dispersion.

6. Conclusions and further work

The dispersion of thermal waves was observed in their propagation processes based on numerical analyses on typical thermal wave modes, i.e. Cattaneo–Vernotte (CV), dual-phase-lagging (DPL), and thermomass (TM). As thermal waves move forward, many peaks appear in the rear of thermal waves relative to the propagation direction. The underlying mechanism for the dispersion of the thermal waves is that they can travel faster in the points with higher temperature considering the temperature dependence of the relaxation time. For the CV-waves and DPL-waves, the origins of the dispersion are due to both the inertia term of heat flux to time ($\tau_q \frac{\partial q}{\partial t}$). For the TM-waves, the origins are due to the inertia term of heat flux to time, inertia term of temperature to time and inertia term of heat flux to space in the TM model, and effects of the inertia term of temperature to space on the dispersion can be neglected, where the inertia term to space comes from the nonlocal effects. The dispersion of the TM-waves is mainly dominated by the inertia term of heat flux to time.

In the TM model, the characteristic time τ_{TM} decreases with the increase of temperature, and therefore the dispersion will appear in the propagation process of the TM-wave. If keeping the relaxation time of heat flux τ_q constant, the dispersion of the CV-wave and DPL-wave does not appear in their propagation processes. But for actual materials, if considering that τ_q decreases with the temperature increasing, the dispersion of the CV-wave and DPL-wave will also appear under the appropriate amplitude of heat flux pulse, relaxation times τ_q and τ_T .

Effects of the amplitude of heat flux pulse and the initial temperature on the dispersion of the TM-wave were also analyzed.

The increase of the amplitude of heat flux pulse and the decrease of the initial temperature both can enhance the dispersion of the TM-wave. Besides, effects of the amplitude of heat flux pulse, the relaxation times τ_q and τ_T on the dispersion of the CV-wave and DPL-wave were analyzed. The increase of the amplitude of heat flux pulse and the relaxation time τ_q can both enhance the dispersion of the CV-wave and DPL-wave, while the increase of the relaxation time τ_T will weaken the dispersion of the DPL-wave.

In the further work, we will investigate the effects of the nonlocal behavior on dispersion of the nonlocal thermal wave models, such as the Guyer–Kruhansl model [24,25] and that proposed by Tzou and Guo [26], which should include comparisons with those of the TM model. Besides, the initial-boundary conditions can affect the dispersion of thermal waves, which also needs further study.

Acknowledgements

This work was financially supported by National Natural Science Foundation of China (Nos. 51322603, 51176099, 51136001), Program for New Century Excellent Talents in University, Tsinghua University Initiative Scientific Research Program, and the Tsinghua National Laboratory for Information Science and Technology (TNList) Cross-discipline Foundation.

References

- [1] D.D. Joseph, L. Preziosi, Heat waves, *Rev. Mod. Phys.* 61 (1989) 41–74.
- [2] D.Y. Tzou, Experimental support for the lagging behavior in heat propagation, *AIAA J. Thermophys. Heat Transfer* 9 (1995) 686–693.
- [3] A.E. Kronberg, A.H. Benneker, K.R. Westerterp, Notes on wave theory in heat conduction: a new boundary conduction, *Int. J. Heat Mass Transfer* 41 (1998) 127–137.
- [4] B.Y. Cao, Z.Y. Guo, Equation of motion of a phonon gas and non-Fourier heat conduction, *J. Appl. Phys.* 102 (2007) 053503.
- [5] F. Vazquez, J.A. del Rio, Thermodynamic characterization of the diffusive transport to wave propagation transition in heat conducting thin films, *J. Appl. Phys.* 112 (2012) 123707.
- [6] G. Chen, Ballistic-diffusive heat-conduction equations, *Phys. Rev. Lett.* 86 (2001) 2297.
- [7] F.X. Alvarez, D. Jou, Boundary conditions and evolution of ballistic heat transport, *ASME J. Heat Transfer* 132 (2010) 012404.
- [8] B.Y. Cao, J. Kong, Y. Xu, K.L. Yung, A. Cai, Polymer nanowire arrays with high thermal conductivity and superhydrophobicity fabricated by a nano-molding technique, *Heat Transfer Eng.* 34 (2013) 131–139.
- [9] P. Zhang, M. Murakami, R.Z. Wang, Study of the transient thermal wave heat transfer in a channel immersed in a bath of superfluid helium, *Int. J. Heat Mass Transfer* 49 (2006) 1384–1394.
- [10] J. Fourier, *The Analytical Theory of Heat*, Dove Publications, Inc., New York, 1955.
- [11] P.M. Morse, H. Feshbach, *Methods of Theoretical Physics*, McGraw-Hill, New York, 1953.
- [12] M.P. Vernotte, Les paradoxes de la théorie continue de l'équation de la chaleur, *C.R. Acad. Sci. Paris* 246 (1958) 3154–3155.
- [13] C. Cattaneo, Sur une forme de l'équation de la chaleur éliminant le paradoxe d'une propagation instantanée, *C.R. Acad. Sci. Paris* 247 (1958) 431–433.
- [14] D.Y. Tzou, The generalized lagging response in small-scales and high-rate heating, *Int. J. Heat Mass Transfer* 38 (1995) 3231–3240.
- [15] D.Y. Tzou, A unified field approach for heat conduction from micro- to macro-scales, *ASME J. Heat Transfer* 117 (1995) 8–16.
- [16] Z.Y. Guo, Q.W. Hou, Thermal wave based on the thermomass model, *ASME J. Heat Transfer* 132 (2010) 072403.
- [17] Y. Dong, Z.Y. Guo, Entropy analyses for hyperbolic heat conduction based on the thermomass model, *Int. J. Heat Mass Transfer* 54 (2011) 1924–1929.
- [18] Y. Dong, B.Y. Cao, Z.Y. Guo, General expression for entropy production in transport processes based on the thermomass model, *Phys. Rev. E* 85 (2012) 061107.
- [19] J. Ordóñez-Miranda, J.J. Alvarado-Gil, Exact solution of the dual-phase-lag heat conduction model for a one-dimensional system excited with a periodic heat source, *Mech. Res. Commun.* 37 (2010) 276–281.
- [20] L.Q. Wang, X.H. Wei, Equivalence between dual-phase-lagging and two-phase-system heat conduction processes, *Int. J. Heat Mass Transfer* 51 (2008) 1751–1756.
- [21] B. Straughan, *Heat Waves*, Springer, New York, 2011.
- [22] V.A. Cimmelli, A. Sellitto, D. Jou, Nonlocal effects and second in a nonequilibrium steady state, *Phys. Rev. B* 79 (2009) 014303.

- [23] D. Jou, V.A. Cimmelli, A. Sellitto, Nonequilibrium and second-sound propagation along nanowires and thin layers, *Phys. Lett. A* 373 (2009) 4386–4392.
- [24] R.A. Guyer, J.A. Krumhansl, Solution of the linearized phonon Boltzmann equation, *Phys. Rev.* 148 (1966) 766–778.
- [25] R.A. Guyer, J.A. Krumhansl, Thermal conductivity, second sound, and phonon hydrodynamic phenomena in nonmetallic crystals, *Phys. Rev.* 148 (1966) 778–788.
- [26] D.Y. Tzou, Z.Y. Guo, Nonlocal behavior in thermal lagging, *Int. J. Therm. Sci.* 49 (2010) 1133–1137.
- [27] A. Barletta, E. Zanchini, Hyperbolic heat conduction and local equilibrium: a second law analysis, *Int. J. Heat Mass Transfer* 40 (1997) 1007–1016.
- [28] A. Banerjee, A.A. Ogale, C. Das, K. Mitra, C. Subramanian, Temperature distribution in different materials due to short pulse laser irradiation, *Heat Transfer Eng.* 26 (2005) 41–49.
- [29] C.W. Chang, D. Okawa, H. Garcia, A. Majumdar, A. Zettl, Breakdown of Fourier's law in nanotube thermal conductors, *Phys. Rev. Lett.* 101 (2008) 075903.
- [30] D. Jou, J.C. Vazquez, G. Lebon, Extended irreversible thermodynamics of heat transport a brief introduction, *Proc. Est. Acad. Sci.* 57 (2008) 118–126.
- [31] J. Fan, L.Q. Wang, Analytical theory of bioheat transport, *J. Appl. Phys.* 109 (2011) 104702.
- [32] R.F. Hu, B.Y. Cao, Study on thermal wave based on the thermal mass theory, *Sci. China Ser. E* 52 (2009) 1786–1792.
- [33] M.R. Wang, N. Yang, Z.Y. Guo, Non-Fourier heat conduction in nanomaterials, *J. Appl. Phys.* 110 (2011) 064310.
- [34] T.T. Lam, A unified solution of several heat conduction models, *Int. J. Heat Mass Transfer* 56 (2013) 653–666.
- [35] D.W. Tang, N. Araki, Wavy, wavelike, diffusive thermal responses of finite rigid slabs to high-speed heating of laser-pulses, *Int. J. Heat Mass Transfer* 42 (1999) 855–860.
- [36] B. Shen, P. Zhang, Notable physical anomalies manifested in non-Fourier heat conduction model under the dual-phase-lag model, *Int. J. Heat Mass Transfer* 51 (2008) 1713–1727.
- [37] C. Herring, Role of low-energy phonons in thermal conduction, *Phys. Rev.* 95 (1954) 954–965.
- [38] J.V. Goicochea, M. Madrid, C. Amon, Thermal properties for bulk silicon based on the determination of relaxation times using molecular dynamics, *ASME J. Heat Transfer* 117 (2010) 012401.
- [39] K. Ramadan, Semi-analytical solution for the dual phase lag heat conduction in multilayered media, *Int. J. Therm. Sci.* 48 (2009) 14–25.
- [40] T.T. Lam, E. Fong, Application of solution structure theorem to non-Fourier heat conduction problems: analytical approach, *Int. J. Heat Mass Transfer* 54 (2011) 4796–4806.
- [41] T.T. Lam, E. Fong, Heat diffusion vs. wave propagation in solids subjected to exponentially-decaying heat source: analytical solution, *Int. J. Therm. Sci.* 50 (2011) 2104–2116.
- [42] C.Y. Wu, Integral equation solution for hyperbolic heat conduction with surface radiation, *Int. Commun. Heat Mass Transfer* 15 (1988) 365–374.
- [43] R. Shirmohammadi, Temperature transients in spherical medium irradiated by laser pulse, *Int. Commun. Heat Mass Transfer* 35 (2008) 1017–1023.
- [44] K.J. Hays-Stang, A. Haji-Sheikh, A unified solution for heat conduction in thin films, *Int. J. Heat Mass Transfer* 42 (1999) 455–465.
- [45] D.W. Tang, N. Araki, Non-Fourier heat conduction behavior in finite mediums under pulse surface heating, *Mater. Sci. Eng. A* 292 (2000) 173–178.
- [46] S. Torii, W.J. Yang, Heat transfer mechanisms in thin film with laser heat source, *Int. J. Heat Mass Transfer* 48 (2005) 537–544.
- [47] M.T. Xu, J.F. Guo, L.Q. Wang, L. Cheng, Thermal wave interference as the origin of the overshooting phenomenon in dual-phase-lagging heat conduction, *Int. J. Therm. Sci.* 50 (2011) 825–830.
- [48] J. Ordóñez-Miranda, J.J. Alvarado-Gil, Thermal wave oscillations and thermal relaxation time determination in a hyperbolic heat transport model, *Int. J. Therm. Sci.* 48 (2009) 2053–2062.
- [49] T.T. Lam, Thermal propagation in solids due to surface laser pulsation and oscillation, *Int. J. Therm. Sci.* 49 (2010) 1639–1648.
- [50] Y. Chou, R.J. Yang, Two-dimensional dual-phase-lag thermal behavior in single-/multi-layer structures using CESE method, *Int. J. Heat Mass Transfer* 52 (2009) 239–249.
- [51] S.M. Yang, W.Q. Tao, *Heat Transfer*, Higher Education Press, Beijing, 2006.
- [52] B.L. Wang, J.C. Han, Y.G. Sun, A finite element/finite difference scheme for the non-classical heat conduction and associated thermal stresses, *Finite Elem. Anal. Des.* 50 (2012) 201–206.
- [53] D. Jou, A. Sellitto, Focusing of heat pulses along nonequilibrium nanowires, *Phys. Lett. A* 374 (2009) 313–318.
- [54] D.Y. Tzou, Nonlocal behavior in phonon transport, *Int. J. Heat Mass Transfer* 54 (2011) 475–481.